GEOLOGICA CARPATHICA, AUGUST 2018, 69, 4, 365–381 doi: 10.1515/geoca-2018-0022

Nucleation and amplification of doubly-plunging anticlines: the Butkov pericline case study (Manín Unit, Western Carpathians)

DUŠAN PLAŠIENKA[1,✉], VIERA ŠIMONOVÁ[2] and JANA BUČOVÁ[3]

[1]Department of Geology and Paleontology, Faculty of Natural Sciences, Comenius University, Mlynská dolina, Ilkovičova 6, 842 15 Bratislava, Slovakia; ✉dusan.plasienka@uniba.sk
[2]Department of Geography and Geology, Faculty of Natural Sciences, Matej Bel University, Tajovského 40, 974 01 Banská Bystrica, Slovakia; viera.simonova@umb.sk
[3]Earth Science Institute, Slovak Academy of Sciences, Dúbravská cesta 9, P.O. Box 106, 840 05 Bratislava, Slovakia; jana.bucova@savba.sk

(Manuscript received January 16, 2018; accepted in revised form May 31, 2018)

Abstract: The Manín Unit represents a transitional tectonic element between the Central Western Carpathians and the Pieniny Klippen Belt. The overall map-view structure of the Manín Unit is dominated by elliptical antiforms composed of comparatively competent Jurassic and Lower Cretaceous strata, surrounded by soft Upper Cretaceous shales, marls and sandstones. During layer-parallel shortening, the Manín sedimentary succession behaved as a multilayer reinforced by a variously thick rigid layer of massive Urgonian limestone. The multilayer deformed by flexural slip folding, but the fold wavelength was controlled by the rigid layer undergoing buckling. It is inferred that, besides the lateral thickness differences in the rigid layer, development of brachyfolds and particularly periclines such as the Butkov fold also resulted from the interference of two perpendicular macroscopic fold systems.

Keywords: Western Carpathians, Pieniny Klippen Belt, Manín Unit, noncylindrical macrofolds, Butkov pericline, structural analysis.

Introduction

The Carpathian Pieniny Klippen Belt (PKB) is characterized by an extremely complex structure from the point of view of the number of lithologically variable tectonic units, as well as their deformation history. In the traditional meaning, the "klippen tectonic style" is the specifically characteristic feature of the PKB, whereby stiff blocks of various dimensions — the "klippen" — are embedded in a soft matrix forming the klippen "mantle" (e.g., Stur 1860; Neumayr 1871; Uhlig 1903, 1904; Andrusov 1938, 1968, 1974; Scheibner 1961; Książkiewicz 1977; Birkenmajer 1986; Maheľ 1981, 1989). Consequently, the PKB was often described in terms of a chaotic block-in-matrix structure — such as the tectonic mélange, megabreccia, strongly boudinaged zone, contracted archipelago, row of diapiric antiforms, huge olistostrome etc. However, this is not a general rule and many sectors of the PKB exhibit a typical fold-and-thrust structure that was subsequently affected and locally disintegrated by out-of-sequence thrusting, transpression and backthrusting (e.g., Ratschbacher et al. 1993; Kováč & Hók 1996; Marko et al. 2005; Plašienka 2012a, b; Pešková et al. 2012; Plašienka & Soták 2015).

Here we provide arguments that conspicuous morphological elevations in the Manín Unit are not klippen in the classic sense, but represent projecting cores of large-scale, doubly-plunging anticlines that still maintain the stratigraphic continuity with the overlying softer strata. In particular, we describe in detail the morphology of the Butkov brachyanticline (pericline), which is the best example of such structures in the Western Carpathians. In addition, we present a tentative model of development of brachyfolds controlled by the rheology of folded strata and/or by interference of two perpendicular fold systems.

Geological situation

The biggest exposure of the Manín Unit occurs in the Middle Váh River Valley of western Slovakia (inset in Fig. 1). It forms an independent tectonic element cropping out in a SW–NE trending zone about 30 km long and up to 5 km wide, being overridden by the frontal elements of the Fatric Krížna Nappe from the SE and bounded by the Klape Unit in the NW (Fig. 1). The area is mildly mountainous with outstanding hills Manín, Butkov and Drieňovka, which represent cores of elliptical, doubly-plunging anticlines composed of comparatively hard Jurassic–Lower Cretaceous limestone formations, as well as several smaller antiforms (e.g., Holiak, Skalica, Bôrová hôrka — Fig. 1) surrounded by depressions filled with Upper Cretaceous marls, shales and sandstones. The W–E trending lens-shaped core of the Butkov pericline forms a crest about 6 km long and 1–2 km wide with several partial hills gradually rising from both sides (Dúbrava and Kalište from the W and

Hradište and Tlstá hora from the E) to the apical Butkov summit (765 m a.s.l.). The Butkov anticline is transversally cut by two deep antecedent valleys of the Lúčkovský and Slatinský potok streams, while the Manín and Drieňovka anticlines are incised by the Manínsky potok brook.

In its whole extent, the Manín Unit only includes Jurassic to Cretaceous, generally continuous strata succession (Fig. 1). The detailed litho-biostratigraphy can be found in a range of publications (Borza et al. 1987; Michalík & Vašíček 1987; Žítt & Michalík 1988; Michalík 1994; Rakús & Hók 2005; Mello ed. 2011; Michalík et al. 2012, 2013). For the purpose of this structurally-oriented paper, the lithostratigraphy of the Manín Unit is simplified into several sequences in order to define their mechanical properties and to visualize the regional structure in a map view (Fig. 1). In the Butkov area, the lower, comparatively thick sequence is composed of Lower Jurassic syn-rift formations consisting of mostly thick-bedded sandy-crinoidal limestones. The post-rift, relatively thin Middle–Upper Jurassic hemipelagic sequence is characterized by red nodular limestones inserted by a thin layer of radiolarites. The Lower Cretaceous part of the Butkov succession consists of the maiolica-type marly and cherty limestones, overlain by massive bioclastic, Urgon-type limestones. This limestone-dominated Butkov succession is followed by a hardground that records a rapid drowning of the Urgonian carbonate platform during the Albian.

The Jurassic–Lower Cretaceous sedimentary succession in the Manín straits slightly differs from that in the Butkov area, the Manín succession being more shallow-water compared to the Butkov succession. In the Jurassic succession, red sandy-crinoidal and condensed nodular limestones prevail over cherty and marly limestones, and radiolarites are missing (Rakús 1997; Mello ed. 2011). Massive Urgon-type limestones are thicker and were deposited in a more proximal position to the platform margin compared to the Butkov area (upper slope to fore-reef; cf. Fekete et al. 2017).

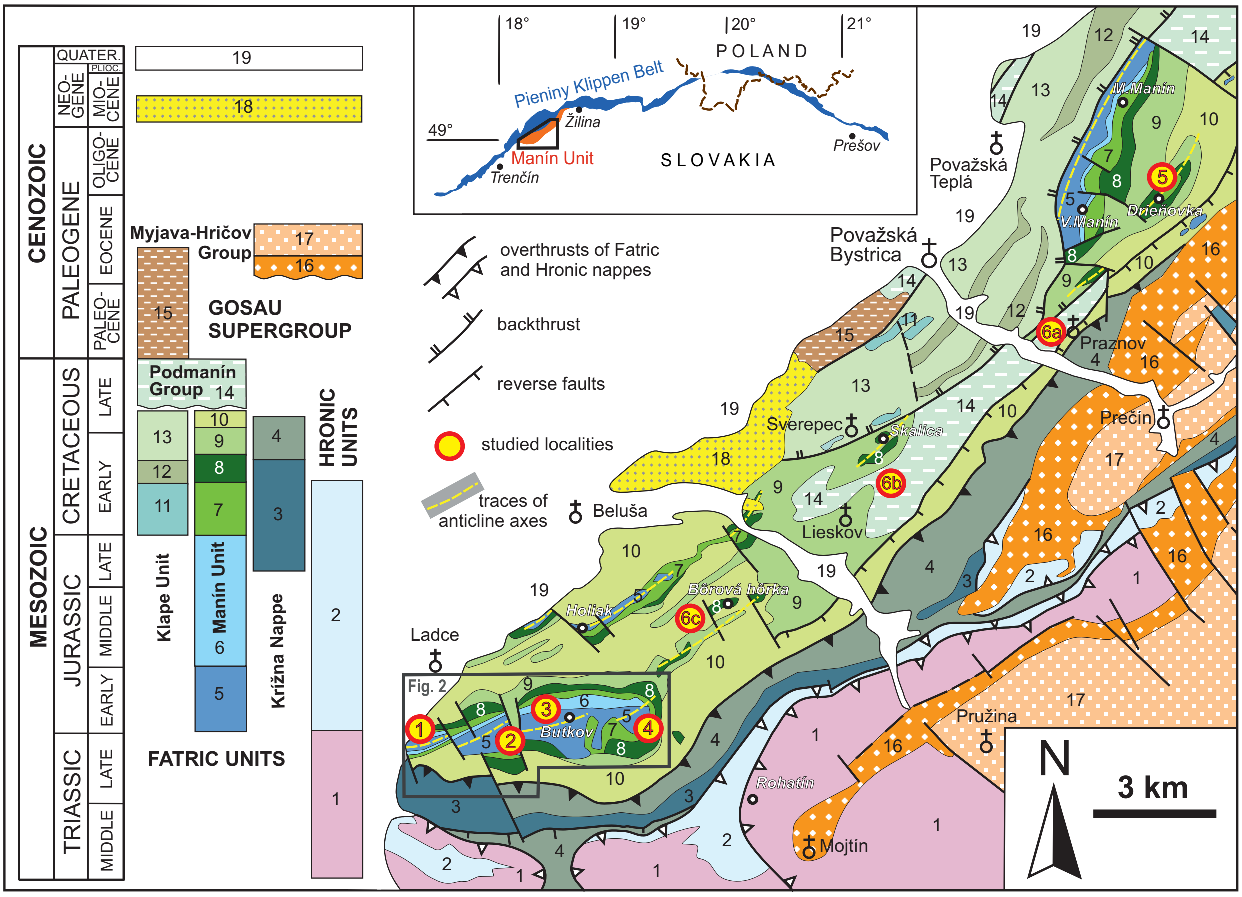

Fig. 1. Geological map of the southern part of the Manín Unit on the left bank of the Váh River, simplified after Mello ed. (2005). Inset shows the geographical position of the Pieniny Klippen Belt and Manín Unit. **Hronic units**: 1 — Triassic carbonate complexes of the Homôľka and Ostrá Malenica nappes; 2 — Jurassic and Lower Cretaceous formations of the Homôľka nappe; **Fatric Križna nappe**: 3 — Upper Jurassic to Lower Cretaceous formations; 4 — Mid-Cretaceous (Albian–Cenomanian) flysch deposits; **Manín Unit**: 5 — Lower Jurassic strata; 6 — Middle–Upper Jurassic succession; 7 — Lower Cretaceous limestones; 8 — Urgonian limestone (Aptian–lower Albian); 9 — Mid-Cretaceous (Albian–Cenomanian) shales and distal flysch deposits; 10 — Upper Cretaceous (Cenomanian–Turonian) proximal flysch with conglomerates; **Klape Unit**: 11 — Neocomian (Berriasian–Barremian) marly limestones; 12 — Aptian marls; 13 — Albian–Cenomanian flysch; **Gosau Supergroup**: 14 — Senonian Podmanín Group; 15 — Paleocene to Lower Eocene Hoštiná succession; 16 — Lower Eocene Súľov Fm.; 17 — Middle Eocene Domaniža Fm.; **Overstep**: 18 — Miocene sediments; 19 — Quaternary fluvial deposits.

The overlying Mid-Cretaceous (Albian–Turonian), hemipelagic to deep-marine clastic, predominantly turbiditic deposits (so-called flysch) represent a new, syn-orogenic sedimentary cycle. The lower Albian hardground is succeeded by hemipelagic marlstones that pass gradually into calcareous turbidites showing a thickening-and-coarsening-upward trend. In the upper parts, bodies of coarse-grained conglomerates and pebbly mudstones with "exotic" clastic material occur.

In the central part of the area, a complex synclinal zone (Lieskov–Praznov syncline in Fig. 1) is filled with the Senonian (Coniacian–Maastrichtian) sediments of the Podmanín Group (Marschalko & Kysela 1980; Kysela et al. 1982; Plašienka & Soták 2015). It is composed of alternating deep- and shallow-marine clastics, hemipelagic variegated marls of the "couches rouges" facies, and calcareous turbidites with exotic conglomerates and rudist reef bodies.

Paleogene deposits do not occur directly within the Manín Unit, but are present in the adjacent Klape Unit, where they fill narrow synclines together with Senonian strata (Hoštiná succession of the Myjava–Hričov Group — Salaj 2006; Plašienka & Soták 2015). The new sedimentary cycle is represented by the Lower Eocene transgressive conglomerates of the Súľov Fm. and Lutetian deepening sequence of hemipelagic variegated shales and turbiditic sandstones of the Domaniža Fm. (Fig. 1; see Soták et al. 2017 and references therein). The Lower–Middle Eocene sediments are confined to the frontal elements of the Central Carpathian Fatric (Krížna) and Hronic cover nappe systems (Fig. 1).

Methods

We have investigated the southern and central part of the Manín Unit in the Middle Váh Valley by means of field-based mesoscopic structural analysis and detailed mapping of selected areas with complicated structure. Most of the structural data were gathered in several large quarries, especially in the Butkov Hill area. In this contribution, we are focused on interpretation of the map-scale fold-thrust structures, using preferably the bedding attitudes, bedding-parallel slickenlines and small-scale folds. Post-folding brittle deformation elements, like faults and slickensides are not treated here, since they have already been analyzed in detail by Šimonová & Plašienka (2011, 2017). The relevant oriented data were processed and visualized by the softwares Stereonet 9.8.3 (© by R.W. Allmendinger, 2011–2016) and WinTensor (© Damien Delvaux; http://www.damiendelvaux.be/Tensor/WinTensor/win-tensor.html). All presented structural attitudes signify the dip direction/dip in degrees (°).

Geometry of macrofolds

Thanks to four large quarries that nicely expose the main features of the Butkov structure in its four main segments (sites 1–4; Figs. 1 and 2), its overall geometry can be comprehensively described. In general, this doubly-plunging anticline (i.e. brachyanticline or pericline) is slightly asymmetric, with steeper northern and gentler southern limb, cut by a system of transversal tear faults with mainly dextral offsets. In the cross-section, the Butkov anticline is closed with the inter-limb angle of ca 60°. In the kinematic interpretation of the macrostructure of the Manín Unit below, we rely on the Butkov pericline in particular, since other localities are not so well exposed and accessible. Site 5 includes fold structures in the central part of the Manín Unit — the large, but incomplete Manín pericline and its satellite Drieňovka pericline (Fig. 1). Additional structural data were obtained also from other localities in the southern part of the Manín Unit, particularly from the complex synclinal structure filled with Senonian strata between Lieskov and Praznov villages. Infrequent and scattered outcrops in this area are collectively described as site 6.

Site 1 — quarry Tunežice

The active, five-level quarry Tunežice is located in the westward narrowing part of the Butkov anticline (Dúbrava segment; Fig. 2), just above the Váh River Valley (GPS coordinates of the centre of the quarry 49°01'09" N, 18°17'24" E). The quarry exposes Lower Jurassic formations of the Butkov Succession, which shape a large-scale, slightly asymmetric anticline with a flatly rounded hinge zone (Fig. 3A), a steeper north-western limb and a gentler south-eastern limb. The calculated fold π-axis is gently SW-plunging and the axial trend of this western segment of the Butkov pericline is SW–NE (Fig. 2B).

Site 2 — old quarry Kalište

The Kalište abandoned quarry occurs on the left (western) side of the Lúčkovský potok Valley (Fig. 2; 49°01'11" N, 18°18'49" E). This valley divides the Butkov anticline into two main parts — the western Kalište segment is complicated by the local synform filled with Cretaceous strata cropping out just in the quarry, while the eastern part is formed by the main Butkov segment with culmination of the pericline crest. The valley follows a steep fault zone (Lúčkovský potok fault zone), in the map scale of roughly NNW–SSE (ca. 160°) strike, which separates the Kalište and Butkov segments (Michalík & Vašíček 1987).

The exposure is dominated by a single discrete, NNW–SSE trending, nearly vertical fault plane covering several tens of square metres of the high quarry wall (Fig. 3B). Large subhorizontal wavy ridges and grooves occur on the fault plane, which together with striations indicate dextral strike-slipping along the fault. Considering parallelism of the fault strike with the orientation of compression and shortening direction during growth of the Butkov fold, this fault has a character of a transfer or tear fault that accommodates a slightly different mode and degree of shortening between the two segments of the Butkov pericline.

Site 3 — quarry Ladce

The huge active quarry (15 levels) exposes a large part of the northern slope of Butkov Hill, which occupies a central position in the Butkov pericline, being located in its core and northern limb (Figs. 1, 2; 49°01'29" N, 18°19'30" E). The lithostratigraphy, embracing the entire Butkov succession from the Lower Jurassic up to Albian strata, was described in detail in numerous papers (Borza et al. 1987; Michalík & Vašíček 1987; Rakús & Hók 2005; Mello ed. 2011; Michalík et al. 2012, 2013). The overall cross-sectional shape of the Butkov anticline was depicted for instance by Michalík & Vašíček (1987), Žítt & Michalík (1988) and Michalík et al. (2013).

Being located in the steeper northern limb of the Butkov anticline, the stratification is constantly NNW-dipping at angles 50–80° (Figs. 2C, 3D). The mean dip is 344/72. A few measurements with opposite dips (Fig. 2C) come from natural outcrops on the southern slopes of Butkov Hill, it means from the south-eastern limb of the anticline.

Numerous slickenlines developed on the bedding planes document the flexural slip mechanism of the Butkov macrofold evolution (Fig. 4). These are predominantly normal to the macrofold axis, but sometimes a succession of superimposed bedding-parallel slickenfibres and striations can be documented with those parallel to the bedding dips being the youngest. An older set is moderately plunging either to

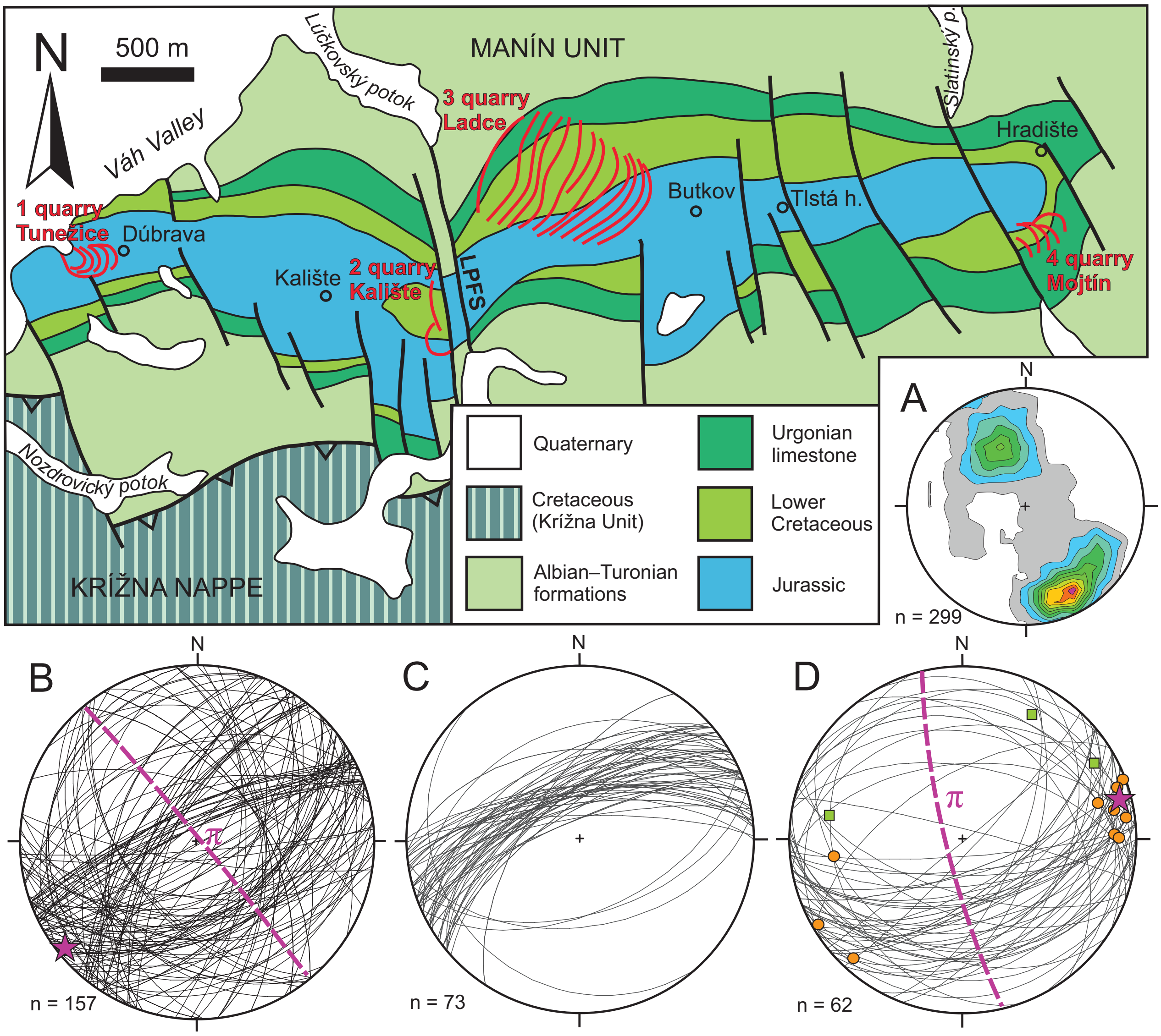

Fig. 2. Simplified geological map of the Butkov pericline with four investigated quarries shown in red (sites 1–4). Map modified after Michalík & Vašíček (1987). Stereographic plots demonstrate the bedding attitudes in the lower hemisphere, equal area projection: **A** — contour diagram of poles to bedding from the whole area (sites 1–4); **B** — great circles of bedding planes with constructed π-circle and π-pole (asterisk), quarry Tunežice (site 1); **C** — great circles of bedding planes, quarry Ladce (site 3); **D** — quarry Mojtín (site 4): great circles of bedding planes with constructed π-circle and π-pole, measured axes of minor folds (green squares) and ß-axes constructed as intersections of fold limb couples (orange circles). LPFS — Lúčkovský potok fault system. Short red lines outline the quarry levels.

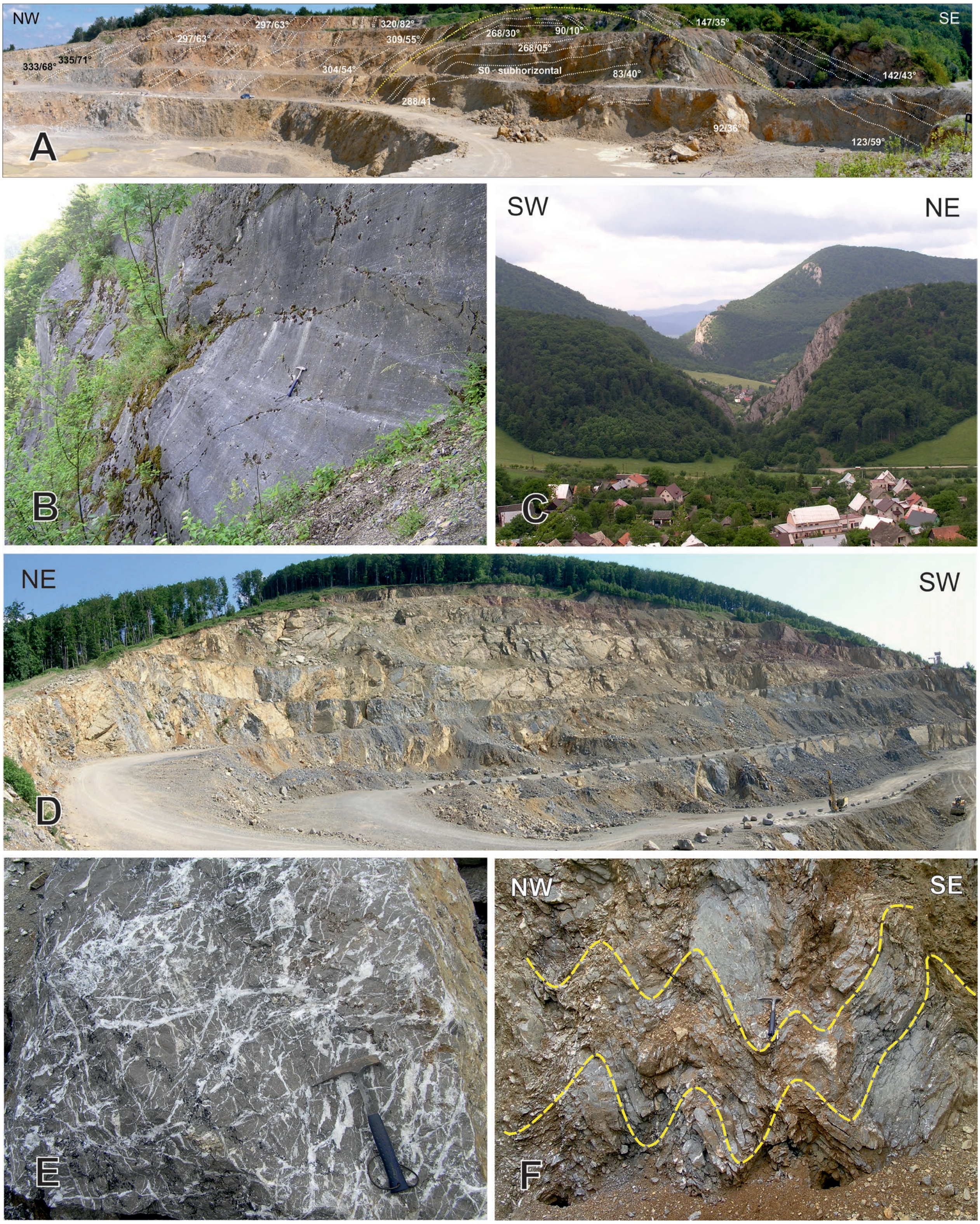

Fig. 3. Phototable of some characteristic structures of the Manín Unit: **A** — scenery of the quarry Tunežice (site 1) exposing a gentle anticline in Jurassic strata; **B** — fault plane of the Lúčkovský potok transfer fault system with horizontal slickenlines in the old quarry Kalište (site 2); **C** — view to the NW into the antecedent valley of the Manínsky potok incised in the Drieňovka (first coulisse, site 5) and Manín (second coulisse) antiforms, Kostolec village in the foreground; **D** — panoramic view from the north of upper stages of the Ladce quarry (site 3) showing en face bedding planes in the northern limb of the Butkov anticline that are steeply NW-dipping; **E** — dense irregular system of calcite veins in the massive Urgonian limestones, quarry Mojtín (site 4); **F** — minute chevron-type folds in the core of the Manín antiform, quarry Mojtín (site 4).

the NW in the western, or to the NE in the eastern part of the quarry, whereas the oldest set is almost horizontal and nearly parallel to the macrofold hinge (Fig. 4B,C,D). These relationships are interpreted in terms of development stages of the Butkov pericline. For this interpretation, we have applied the model by Price & Cosgrove (1990, p. 465; modified in Fig. 4A), whereby amplification of non-cylindrical, elliptical antiforms is recorded by sets of crosscutting, bedding-parallel slickenlines that represent increments of the fold amplification. Initially, points X and Z (stage 1) are located close to the ends of the pericline and fibres develop at angle α approximating 0° to the fold hinge. As the pericline grows, points X and Z move closer to its central part and angles α_1 are oriented obliquely to the hinge (stage 2). Finally, when points approach the pericline centre, the youngest generation of slickenfibres develop at right angles to the pericline hinge (stage 3 in Fig. 4). Note that point Z moved eastward slightly beyond the centre in this particular case.

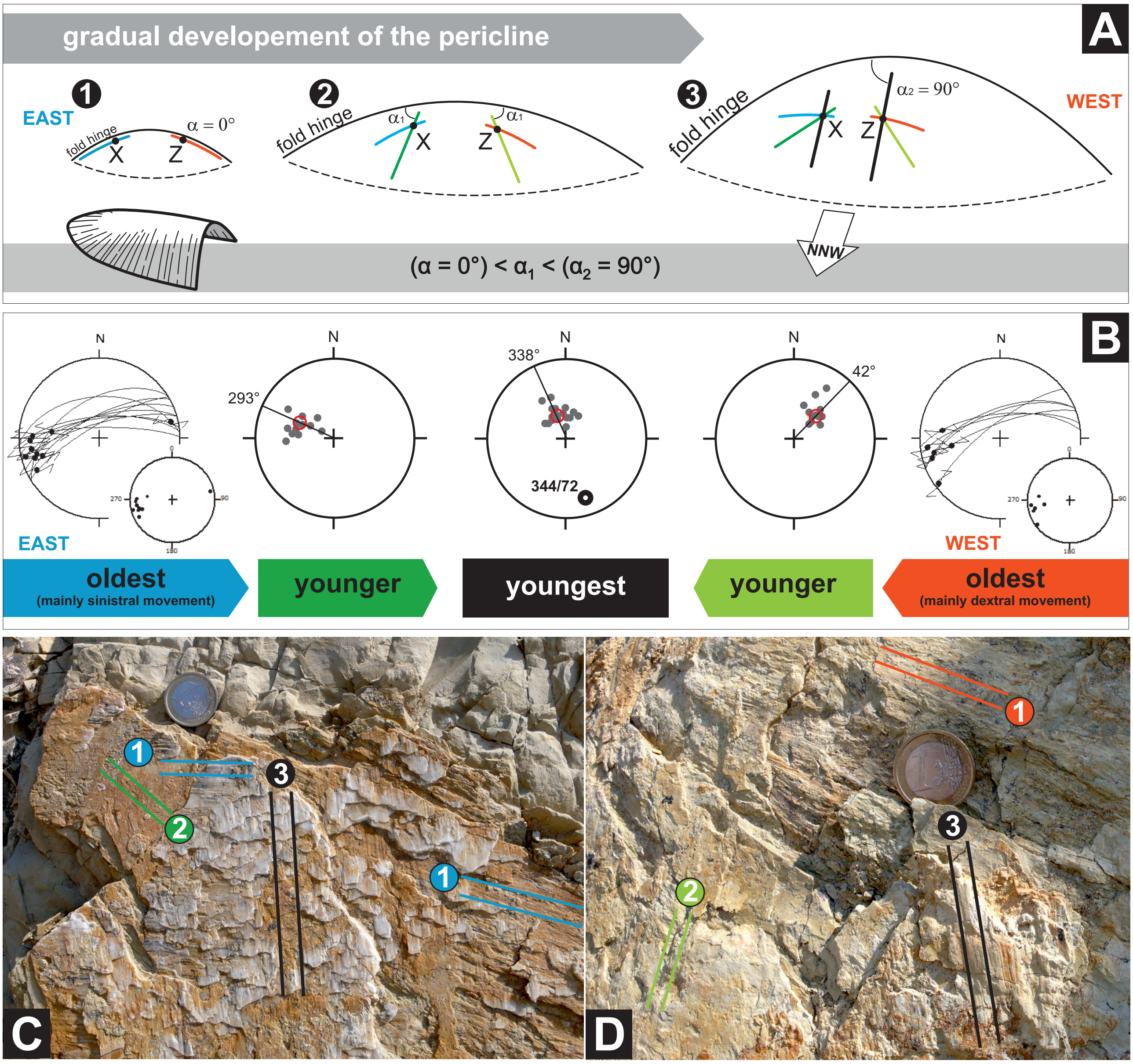

Fig. 4. Growth stages of the Butkov pericline as inferred from superposition of slickenlines developed on the bedding planes in the Ladce quarry (site 3). Adapted from Bučová (2013). The panel **A** outlines the sequential growth of the brachyanticline with progressive development of crosscutting slickenlines according to Price & Cosgrove (1990). Note that scheme is viewed from the north like the quarry view in Fig. 3D. **B** — peripheral stereograms depict the bedding great circles and bedding-parallel striations indicating the opposite sense of flexural slips in the western (red) and eastern (blue) parts of the Ladce quarry, it means approaching the westward and eastward plunging hinges of the Butkov pericline, respectively. The central diagram shows striation traces and the mean direction of the youngest population of slickenlines, and the average pole to bedding 344/72, while the side plots represent the intermediate stages. The photographs illustrate examples of crosscutting slickenlines on the bedding planes.

Site 4 — quarry Mojtín

The large, 7-stage active quarry is located on the right side of the Slatinský potok Valley, between Belušské Slatiny and Mojtín villages. The valley follows a transversal fault that separates the eastern Hradište segment from the central part of the Butkov pericline (Fig. 2; 49°01'11" N, 18°21'34" E). From the structural point of view, the quarry exposes the south-eastern limb of the eastern conical closure of the Butkov brachyanticline, thus it completes information about the general construction of this dominant macrostructure of the region. The entire Middle Jurassic–Lower Cretaceous Butkov Succession is exposed in the quarry. Massive Urgonian limestones crop out in the eastern parts of the quarry levels, westward they are underlain by older, thinly-bedded to schistose Upper Jurassic to Lower Cretaceous marly limestones.

Small-scale structures that are presumably related to the pre-folding and probably syn-emplacement deformation are preferably preserved in marly lithologies. Bedding-parallel, anastomozing solution seams in schistose and stylolites in more massive limestones indicate flattening normal to stratification. The scaly fabric, occasionally with structures indicating non-coaxial shearing parallel to the stratification, along with sporadic traces of cleavage oblique to bedding, may record the thrusting event, as interpreted by Prokešová et al. (2012) in the Fatric Krížna nappe. Part of the early syntectonic calcite veins could have been related to the thrusting process, too.

The rocks in the quarry are penetrated by several generations of syn- to post-tectonic calcite veins. These were studied in detail already by Mišík (1966), who distinguished veins with blocky or fibrous calcite fillings, the antitaxial fibrous veinlets being the most common. According to macroscopic observations in the quarry, most of calcite veins can be characterized as pre- or early syntectonic with respect to formation of the Butkov macrofold. The massive Urgon-type limestones contain a dense network of irregular, short and variously thick veins filled with blocky calcite (Fig. 3E). These indicate a fluid overpressure in time of their formation. Well-bedded strata show a fairly regular system of bedding-normal veins, partially with fibrous fillings, which were probably formed during the early stages of the macrofold development by flexural folding as the extensional longitudinal fractures. They were later segmented in the fold limbs by the layer-parallel flexural slipping. Some of the veins formed obviously by opening of earlier cleavage planes, utilizing weak zones of pre-existing pressure solution seams, whereas some others are cut by younger stylolites.

In places in the core of the macrofold, the thinly-bedded to schistose Lower Cretaceous marly limestones are contorted by minute folds (Fig. 3F). Folds are mostly of chevron type, symmetrical with straight limbs and angular hinges; the interlimb angle varies between 80 and 50°. Axial planes are prevailingly vertical, or steeply NW- or SE-dipping. Measured fold axes and constructed π- and β-axes are gently plunging chiefly towards the ENE (Fig. 2D).

Site 5 — Manín and Drieňovka gorges

The Manín Narrows are one of the most spectacular limestone gorges in western Slovakia. Its narrowest parts are incised in the massive Urgonian limestones of central part of the Manín pericline. One km to the SE, the same valley cuts another, but smaller pericline named the Drieňovka antiform (Fig. 3C; 49°07'55" N, 18°31'23" E).

Whereas the larger Manín pericline is fairly asymmetrical with the northern limb truncated by the steeply NW-dipping reverse fault that developed due to backthrusting of the adjacent Klape Unit, the smaller Drieňovka pericline is an upright, open, nearly angular symmetrical anticline in a cross-section (Fig. 5A). This spectacular structure was drawn and photographed in numerous publications, for example, by Andrusov (1938), or in detail by Rakús (1997). The Drieňovka fold is framed by several tens metres thick competent layer of Urgonian limestone, while the thin-bedded Lower Cretaceous limestones in the fold core are disharmonically folded (Fig. 5B).

The well-bedded Lower Cretaceous strata in the core of the Drieňovka macrofold are distorted by metric to decametric, gentle to open folds with the interlimb angle 70° or more. We have measured the accessible fold limbs especially along the NW flank of the large-scale Drieňovka anticline (Fig. 5B). The poles to bedding are dispersed along a NW–SE oriented great circle with the π-pole 220/7 (Fig. 5C).

Site 6 — Lieskov–Praznov synform

We have performed field structural mapping with measurements of bedding attitudes of various formations at a number of scattered small outcrops in the Lieskov–Praznov synform and in area further SW up to the Butkov anticline (for instance 6A — Praznov area; 6b — Lieskov–Skalica area; 6c — Bôrová hôrka area in Fig. 1). The region is characterized by a complex fold-thrust structure with narrow anticlines formed by competent Jurassic–Lower Cretaceous limestones and broader synclines filled with soft Upper Cretaceous sediments. Macrofold limbs are truncated by steep oblique-slip, reverse-dextral faults. They are dipping in opposite directions along flanks of the Manín Unit — to the SE along its south-eastern margin, while dips to the NW prevail along the north-western boundary with the Klape Unit (area immediately north of village of Lieskov in Fig. 1). This structure is more open in the south-western part of the domain, while the opposite-dipping thrust faults are gradually merging in the NE direction along the regional axial plunge of the Lieskov–Praznov syncline, and finally join together south of the Manín domain. As a result, this NE-ward tapering tip of the Lieskov synform attains a roof-like shape with the synform squeezed in the centre (Fig. 6). The area is complicated also by steep axial undulations, in other words frequent "cross-strike" bedding attitudes — gently to steeply dipping either to the SW or less frequently to the NE (see tectonogram in Fig. 6). This pattern also controls the broad-scale geometry of the Lieskov–Praznov syncline, which is then described as a complex brachysyncline. It is inferred that the NW–SE trending bedding strikes resulted from a folding event with W–E to SW–NE oriented shortening. This event should have been older than the SW–NE striking fold-thrust structures that dominate the tectonic edifice of the area, since the NW–SE oriented bedding strikes are mostly preserved in central parts of tectonic imbricates separated by almost straight SW–NE trending oblique reverse faults.

Post-folding structures

A large dataset of more than a thousand post-folding faults and their kinematic and paleostress interpretations from

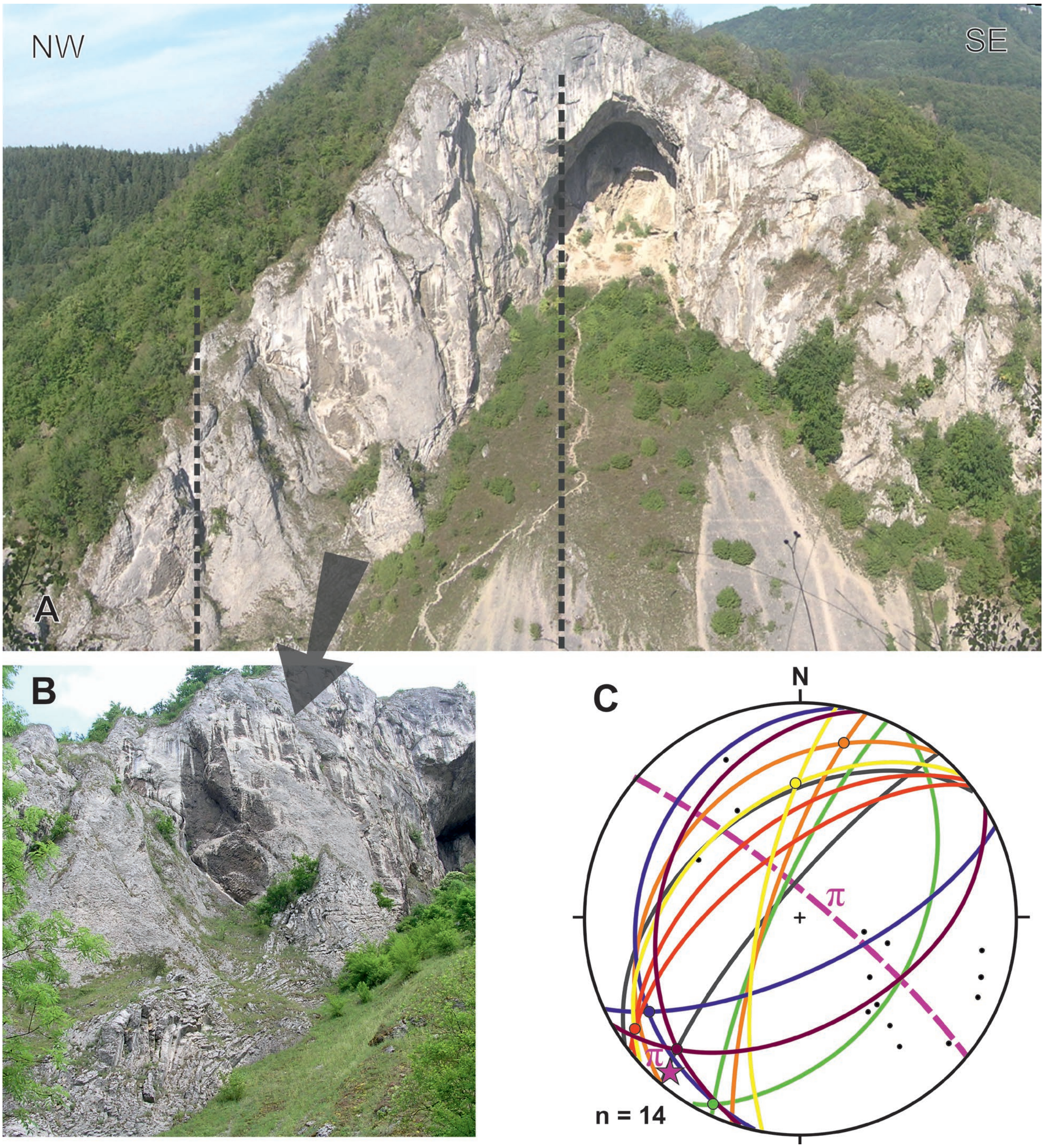

Fig. 5. The Drieňovka anticline: **A** — the fold core framed by a thick layer of competent Urgonian limestone, view to the NE; **B** — subsidiary disharmonic folds in well-bedded Lower Cretaceous limestones forming the northern limb of the anticline core; **C** — stereographic projection of great circles and poles to bedding (black dots), and π-circle with π-pole (asterisk); great circles and β-intersections of fold limb pairs are coloured.

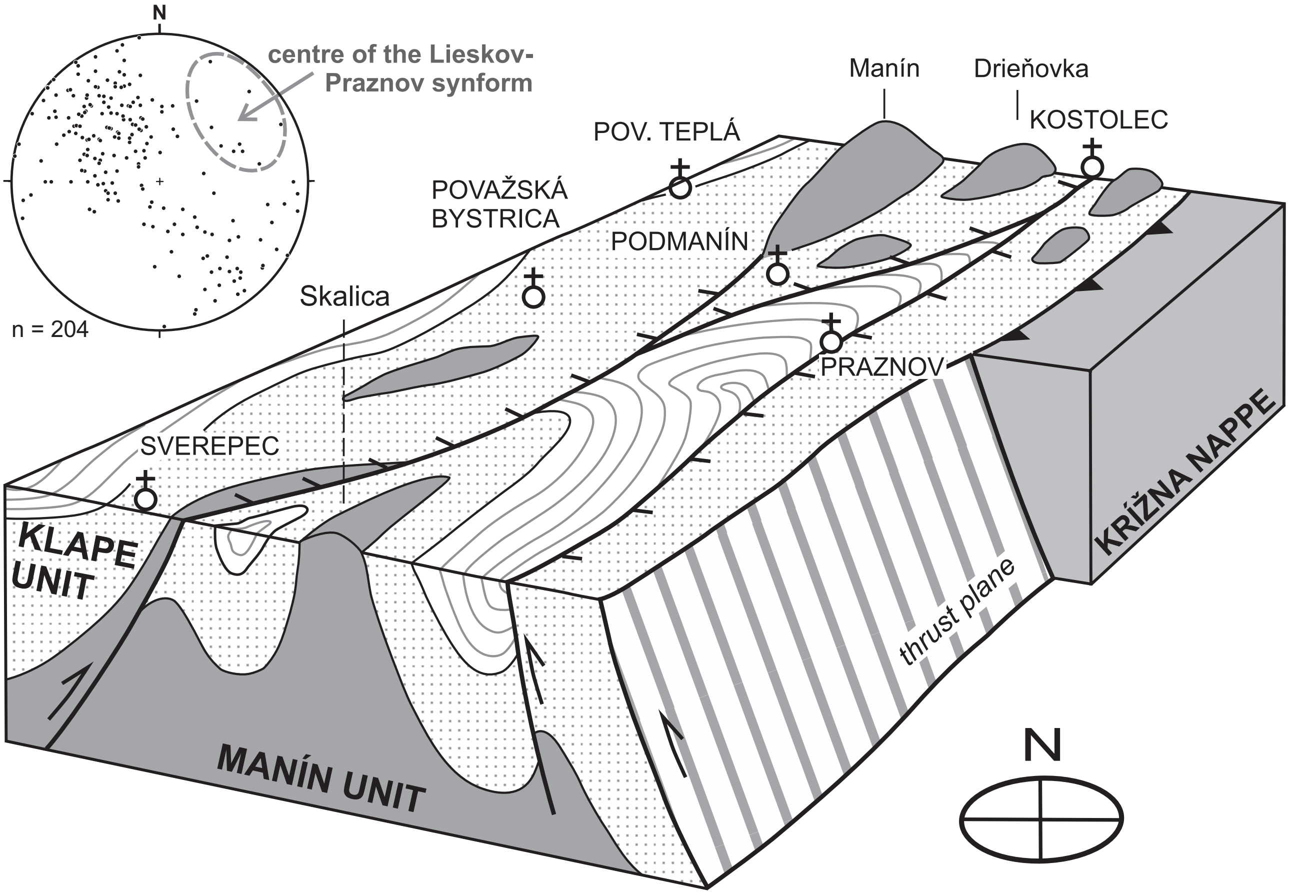

Fig. 6. Block diagram outlining the structural pattern of the Lieskov–Praznov synform. Lower Cretaceous limestone formations are shown in grey, Mid-Cretaceous flysch sequence is stippled and Senonian Gosau deposits in the centre of the synform are hachured to show the bedding strikes. The stereographic diagram plots the poles to bedding. Note that the transversal steeply SW-dipping bedding planes prevail in the middle and NE part of the Lieskov–Praznov synform.

the Butkov quarries were published by Šimonová & Plašienka (2011, 2017). The paleostress interpretation has had to take into account the measured ca 50°–60° CCW rotation of the Western Carpathian part of the AlCaPa megablock during the late Early and early Middle Miocene (e.g., Márton et al. 2013, 2015). Considering this, the relationships of the pre-, syn- and post-rotation brittle fault structures in the whole Manín Unit have been evaluated and interpreted by Šimonová & Plašienka (2017). Consequently, all the pre-Miocene structural directions presented in this paper should be corrected for this rotation, too.

Discussion

Kinematic framework of the Butkov pericline

In an older opinion of Maheľ (1980, 1983, 1985), the Butkov and Manín anticlines represent erected frontal cores of recumbent folds submerging southwards below the main body of the Krížna nappe. However, the geometry of these folds appears to be strongly modified by their post-emplacement amplification, generally by layer-parallel shortening and upright buckle folding of initially flatly lying or moderately folded strata successions of the Manín Unit, together with the overstepping Gosau deposits.

Considering the general context of the structure of the Klippen Belt in the Middle Váh Valley, the Manín Unit, along with the Klape Unit, occupies a position in the rear part of the Paleogene accretionary wedge of the PKB united with the External Carpathian Flysch belt. Being buttressed by the CWC block, the wedge developed as the NW-ward propagating fold-thrust belt that grew by frontal accretion of the Oravic and Magura units. This process commenced shortly after the final nappe emplacement of the Manín and Klape units in the early Senonian and continued during the Paleogene up to Early Miocene (cf. Plašienka & Soták 2015 and references therein). As the wedge grew, its rear parts thickened and were affected by backtilting and backthrusting. Backtilting is evident in the Flysch Belt units adjacent to the PKB (Biele Karpaty and Bystrica units of the Magura Belt), and also in the Klape Unit where strata are steeply NW-dipping and mostly overturned (e.g., Mello ed. 2011; Beidinger & Decker 2016). Backthrusting influenced preferably the backstop area, for example, the Klape and Manín units interface (Fig. 1), the Manín–Krížna contact zone and reached as far as the external CWC zones in the Strážovské vrchy Mts. (Maheľ 1985).

In a cross-section, the Butkov macrofold is an upright, closed to tight, slightly asymmetrical anticline with northern vergency. Formed by flexural folding, this geometry predicts nearly horizontal shortening of a flatly lying sedimentary succession. In general, the Butkov pericline preserves its generally NW-verging geometry from the earlier stages of the accretionary wedge development, but is affected by the local SE-directed reverse faults as well (Michalík & Vašíček 1987). Numerous NW-dipping small-scale reverse and oblique-slip faults and slickensides were revealed by a detailed structural analysis in the Ladce quarry and were interpreted as brittle structures related to the NW–SE to NNW–SSE oriented principal stress axis that operated during the Early Miocene (Šimonová & Plašienka 2011). However, this post-folding brittle deformation has little affected the overall shape of the Butkov pericline.

As described above, the Butkov pericline is segmented by a system of subvertical, NNW–SSE trending faults (Fig. 7). Since these faults separate the pericline segments with a different degree of shortening, they might be considered as transfer (tear) faults. Nevertheless, these faults mostly show a dextral offset, revealed also by the kinematic analysis (site 2). It is inferred that the original transfer faults that developed during the pericline growth were later reactivated as a system of dextral strike-slips that accommodated backthrusting along an oblique ramp formed by rigid Triassic carbonates of the Hronic units to the S-SW of the Butkov fold. Transversal, NW–SE to NNW–SSE striking faults are common in the whole area (Fig. 1).

Origin and growth of the Butkov pericline

In terms of rheological properties that control the folding mechanisms, the Butkov sedimentary succession may be characterized as an approximately two thousand metres thick multilayer composed mostly of well-bedded strata. If subjected to the layer-parallel shortening in semi-ductile style, multilayers are prone to folding by the flexural slip mechanism, as indicated by slickenlines occurring on the stratification planes. In addition, the Butkov fold is framed by a relatively thick competent layer of the Urgonian limestones embedded between the softer underlying multilayer and overlying incompetent shales, marls and turbidites. During layer-parallel shortening of the multilayer, the strong Urgonian layer was deformed by buckling, whereby the initial fold wavelength of the buckled layer was controlled by its thickness and viscosity contrast with respect to the underlying and overlying complexes. Hence we infer that nucleation of the Butkov pericline and other large-scale folds in the Manín Unit was controlled by the initial buckling instabilities within this competent layer. The subsequent fold amplification depended on

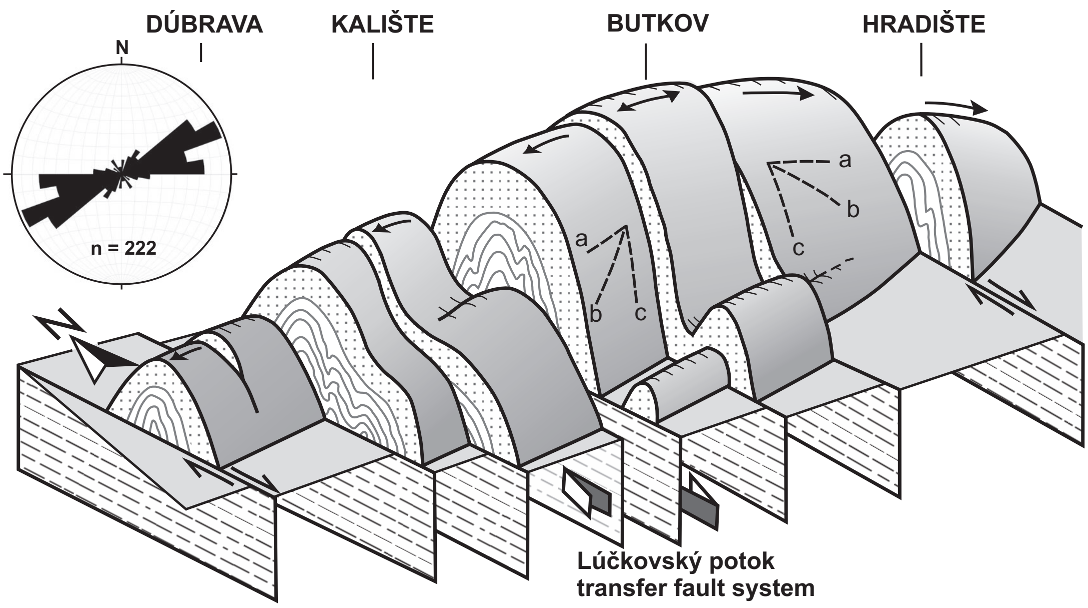

Fig. 7. A perspective view from SW on the geometry of the Butkov pericline constructed for the reference top plane of the Urgonian limestone layer which is dotted in cross-sections. Not to scale. The horizontal cutting plane is at approximately 250 metres altitude above sea level. The pericline is segmented by a set of dextral strike-slip faults, the most prominent being the Lúčkovský potok transfer fault system with distinct horizontal slickenlines (cf. Fig. 3B). Major transfer faults cut the pericline into four main segments — Dúbrava, Kalište, Butkov and Hradište from W to E. Opposite plunges of the fold axis in the hinge zone are shown, with culmination on Mt. Butkov. Traces of sequentially developing bedding-parallel slickenlines, documenting the flexural-slip mechanism and growth stages of the pericline (from “a” as the oldest to “c” as the youngest stage), are schematically indicated as mirrored from the northern limb (cf. Fig. 4). Notice that the post-folding deformation elements, like local reverse and normal faults (e.g., Michalík & Vašíček 1987), are not considered, as well as the present erosional topography is not depicted. The rose diagram shows the general trend of the bedding strikes.

the amount of shortening, and the final overall shape resulted from the degree of augmentation of pre-existing perturbations and/or from overprinting of two orthogonal folding events.

As stated by Dubey & Cobbold (1977), all natural folds are non-cylindrical to a certain extent, being formed by three-dimensional processes of propagation and interference. Hence the question arises how non-cylindrical folds are initiated. Considering the non-cylindrical geometry of the Butkov fold, several possibilities might be assumed in general, which are discussed in the following text: (1) transpression along the SW–NE trending wrench corridor of the PKB, including the Manín Unit; (2) amplification of pre-existing non-cylindrical fold contortions inherited from the thrusting stage; (3) along-strike variations in the amount of shortening perpendicular to the fold axes; (4) development of folds in the constrictional strain field; (5) lateral thickness differences in the competent Urgonian layer acting as non-cylindrical deflections that might amplify during the layer-parallel shortening; (6) interference of two orthogonal or oblique fold systems. Whilst the first five options assume a single-event folding event, the sixth model presumes a superposition of two distinct folding phases.

(1) It is well known from models of transpressional thrust belts or wrench zones (e.g., Sanderson & Marchini 1984; Ratschbacher et al. 1993; Jones et al. 2004; Ruh et al. 2017) that contraction oblique to the wrench zone boundaries, or at restraining bends of such zones, generates en-echelon arrays of non-cylindrical folds confined by the zone walls. This is due to the partitioning of non-coaxial deformation between the dominant strike-slip shearing along the zone walls and the compression dominating inside the zone. However, in this case a different succession of the bedding-parallel slickenlines would be expected — as primary should be those normal to the fold hinge, while secondary slickenlines should be obliquely oriented, due to a gradual rotation of the macrofold hinge towards the wrench zone boundaries. As a result, this would produce an opposite succession as it was observed and documented above. The slight dextral transpression occurred in the area, as documented by the paleostress analysis of fault structures (Šimonová & Plašienka 2011, 2017), but it was superimposed on the fold-thrust structures during the later post-folding stages.

Moreover, the hinge axes of macrofolds in the Manín Unit are generally parallel to its tectonic boundaries, as well as to boundaries of the PKB as a whole. However, obliquity of the fold axes to the zone boundaries would be expected in the transpression model. Apparently, the Butkov pericline seems to be an exception, because it trends W–E in the map view (Figs. 1 and 2), which means oblique to the general SW–NE strike of the Manín Unit and PKB. On the other hand, as shown above, the internal structural trends of the Butkov pericline are still SW–NE trending and the W–E trend of its long axis is putative only, caused by segmentation and dextral translation of the fold core segments along the NNW–SSE striking tear faults (Figs. 1, 2 and 7).

(2) Modification of inherited, thrusting-related recumbent folds (Maheľ 1986) can be ruled out from following reasons: (i) in numerous papers Maheľ argued (e.g., 1983, 1985, 1986) for the close structural relationships of the Manín Unit with the Krížna nappe, including presence of large-scale recumbent folds — "digitations" in both. Nevertheless, most of these digitations, which repeat sedimentary successions, can be interpreted as fault-bend folds and imbricated duplex structures with locally preserved slices containing overturned successions (Prokešová et al. 2012); (ii) as documented above, the Butkov and other anticlines in the Manín Unit were formed by layer-parallel shortening and upright flexural folding of originally flat-lying sedimentary successions. This, however, does not exclude presence of pre-existing, thrusting-related gentle fold contortions that amplified during the main phase of macroscopic folding of the Manín Unit.

(3) Theoretically, a pericline can result from an effect of variation in shortening perpendicular to the fold axis, whereby the axial culmination coincides with the region of maximum shortening (cf. Ramsay & Huber 1987, p. 469, fig. 21.33). In nature, such an effect could be perhaps expected in front of a rounded indenter. However, the regional tectonic pattern of the Manín Unit does not comply with this structural configuration.

(4) The modern numerical modelling techniques suggest that non-cylindrical folds can be formed by a single folding event. However, some specific circumstances are required. Applying viscous rheology in coaxial experiments, initial geometric perturbations of a buckled single layer and/or a constrictional strain field are assumed in a majority of models for single-phase non-cylindrical folding (e.g., Ramsay & Huber 1983, 1987; Schmalholz 2008; Liu et al. 2016). A constrictional setting is well applicable for small-scale folds in ductile media, but can hardly be achieved in outer convex arcs of convergent orogens like in the case of the Manín Unit. As described by Ramsay & Huber (1983, p. 66) the single-phase constrictional contraction causes all folds to be highly irregular in shape, fold axes and axial planes have many different orientations, their intersections and merging are unsystematic. In contrast, superposition of contractions in different phases produces systematic interference geometry and fold axes are more regular in orientation. Therefore Ramsay & Huber (1987, p. 494–495) presented a cautionary note that the current fashion to reinterpret two-phase interference patterns as single phase event might be misleading and careful evaluation is needed to distinguish both.

(5) Lateral thickness differences, together with facies variations of the Urgonian limestones in the Manín Unit are well known. For example, the Urgonian layer reaches up to 200 metres in the broad Manín anticline, but thins to less than 100 metres in the tighter Drieňovka anticline ca. 1 km SE-ward. In the Butkov domain, the layer has some 100 metres, while in the Skalica domain to the NE it does not exceed a few tens of metres (Fig. 8A). This is mainly due to the fact that the Urgon-type limestones are mostly resediments composed of the platform-derived detritus deposited in slope aprons and slope-toe fans (e.g., Fekete et al. 2017). Real bioherms only occur on Mt. Manín, where they represent the most proximal zone at

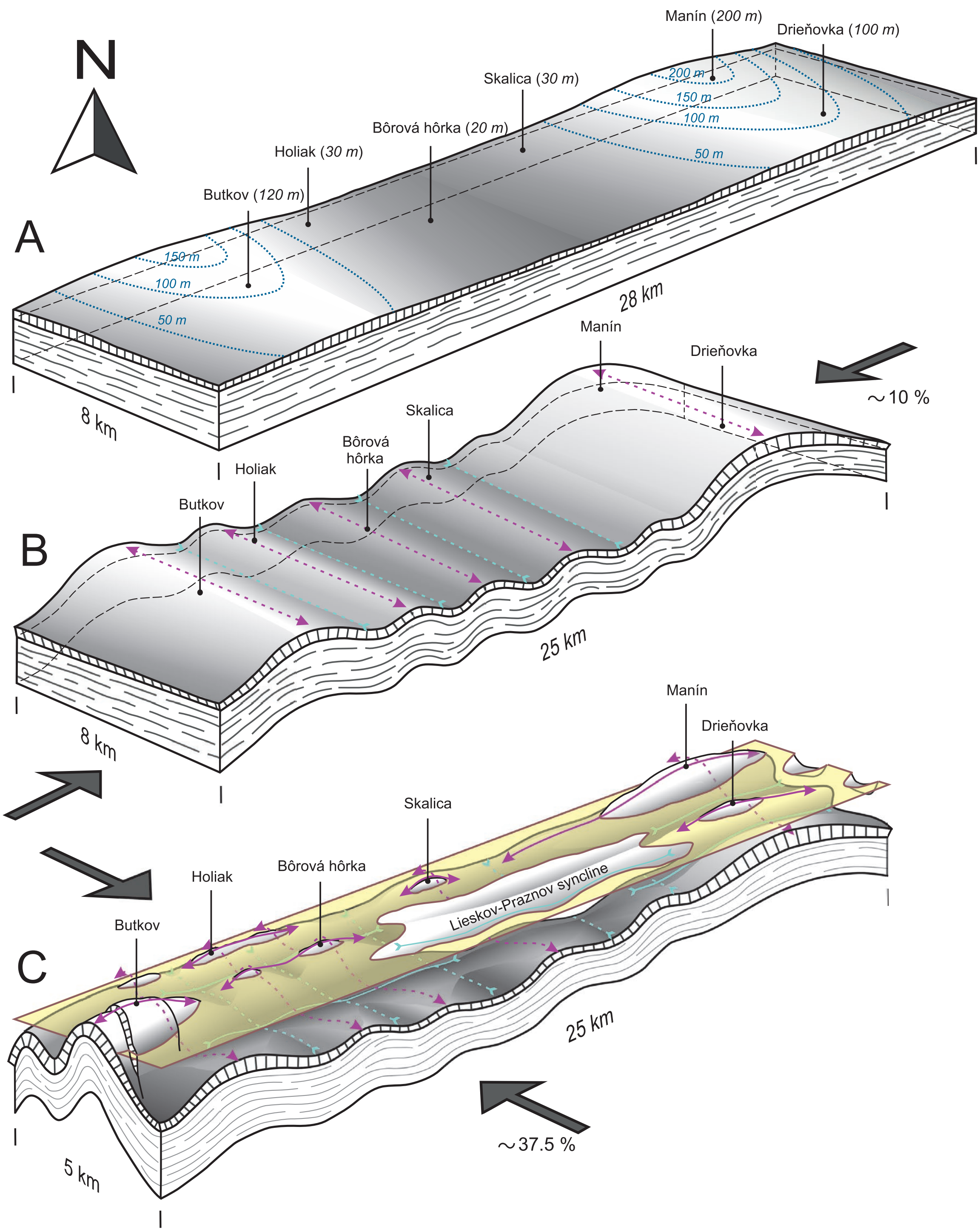

Fig. 8. Block diagrams illustrating the kinematic model of the evolution of macrofold structures in the Manín Unit. Structures are visualized by the shaded upper surface of the vertically ruled, mechanically strong Urgonian layer, the underlying multilayer is horizontally hachured. Grey shading indicates either the small thickness of the Urgonian layer or structural depressions (synclines) by dark tones. **A** — restored pre-deformation state, numbers show thicknesses of the Urgon layer at the main present elevation points (see Fig. 1), blue dotted isolines indicate thickness of the rigid Urgonian limestone layer; **B** — phase of moderate, ca 10 % shortening in W–E to SW–NE direction, first set of NW–SE trending macrofolds developed, anticline axes are indicated by red dotted, arrowed lines, syncline axes are green; **C** — main folding phase with NW–SE contraction and modelled 37.5 % shortening, respective macrofold axes are depicted by solid lines with arrows. The yellow transparent horizontal plane designates an imaginary level surface at ca 400 m a.s.l., which is approximately the mean elevation of the area. Pericline cores go above this plane, whereas the Lieskov–Praznov syncline, delineated by the base of Senonian strata, forms a depression below the level surface. Note that only fold structures are shown, the subsequent contraction resulting in reverse faulting and imbrication, especially in the central part of the model, is not considered. See the text for further explanation.

the carbonate platform edge. The thickness distribution of Urgonian limestones in the Manín Unit generally indicates input of bioclastic material from the north-west in two lobes tapering along- and across-strike — one in the Butkov and second (thicker) in the Manín area (Fig. 8A). This pattern supports an assumption about the paleogeographic position south of an elevated ridge with a prograding Urgonian carbonate platform, most probably the South Tatric Ridge, which supplied bioclastic debrites deposited in the adjacent Zliechov basinal area of the Fatric realm (Michalík 2007).

Sandbox analogue modelling showed that even gentle pre-deformational, along-strike thickness variations of clastic wedges overlying viscous sole produce dramatic changes in structural pattern and kinematic evolution of accreting thrust wedges (Storti et al. 2007). This observation can be partially applied to our case where the lateral thickness differences in the Urgonian limestone layer governed the structural style of the Manín part of the growing amalgamated thrust wedge of the PKB and the External Carpathian Flysch Belt. It can be inferred that the basal lubricant of the detached sedimentary multilayer of the Manín Unit, which is not exposed at the surface, is composed of weak Upper Triassic shales and evaporites of the Keuper Fm. These commonly form the principal décollement horizon for the frontal units of the Fatric nappe system (Prokešová et al. 2012).

We presume that during buckling, primary folds in thinner parts of the rigid layer developed with shorter wavelengths and amplitudes, opposite to the thicker parts. As the folds amplified, growth of the short-wavelength folds was gradually blocked, while the long-wavelength folds tightened and their amplitudes grew far beyond the amplitudes of the initially short-wavelength folds. If the strong layer thickness also diminishes along axes of the large folds, doubly-plunging anticlines could be produced. This can really be documented in the Butkov pericline — Urgonian limestones reach ca 100 metres at its culmination (Butkov-3 site), but considerably decrease below 50 metres toward the axial depressions (sites 1 and 4; Figs. 7, 8A).

In the model by Liu et al. (2016), development of a single-phase periclinal fold set was effectively simulated by introducing periodic perturbations along the fold axis direction supplemented by erosional unloading during the fold growth. Considering this, the thickness variations of the buckled competent layer may represent the initial perturbations that were amplified during unidirectional shortening. On the other hand, the model presumes extensive erosional unloading to achieve the periclinal geometry, which is not supported by the regional structural situation in the Manín Unit, since the Upper Cretaceous sediments overlying the stiff layer are largely preserved, particularly in brachysynclines like the Lieskov–Praznov one. Hence the numerical model of Liu et al. (2016) has a limited applicability to the Butkov and other periclines in the Manín Unit, but might be considered as an alternative (see caption to Fig. 8).

(6) The whole Klippen and Periklippen region is characterized by fold-thrust structures and narrow imbricates that trend parallel or slightly oblique to its boundaries. However, along-strike elevations and depressions also exist, distinctively in our study area with several brachyantiforms (Manín, Drieňovka, Butkov) and brachysynforms like the Lieskov–Praznov synform (Fig. 1; site 6). Especially the latter case indicates that not only the buckling instabilities assumed above might have contributed to the structural pattern of the area. The folding with NW–SE to N–S structural trends indicating SW–NE to W–E compression was documented by structural analysis in several sectors of the PKB, for example, in the Slovak Pieniny Mts. (Plašienka 2012b), or in the Kysuce region (Beidinger et al. 2011; Beidinger & Decker 2016), and were detected in practically all other PKB sectors as well. At an outcrop scale, these structures are indicated by minute folds with weak axial-plane cleavage, which were probably associated with long-wavelength and low-amplitude open folds at the macroscale with estimated at maximum 10 % shortening (Fig. 8B). It is a regional event widely affecting also various units of the inner Carpathians zones (e.g., Plašienka 1983, 1993, 1995a, b, 1999; Plašienka & Marko 1993; Plašienka & Soták 2001), where it is registered mainly by generally N–S trending angular folds and kink bands, usually representing the third deformation stage marked as "cross-folding" (i.e. perpendicular to the dominant structural trend) in the local structural evolutionary schemes. However, this event has not been evaluated from the point of view of the regional kinematic framework yet.

During the superimposed, intense NW–SE to N–S compression and shortening, which was the dominant deformation process in the PKB, the interference of the pre-existing NW- to N-trending folds and newly developing along-strike trending folds could have produced the type 1 fold interference pattern (e.g., Ramsay 1967; Ramsay & Huber 1987; Odonne & Vialon 1987; Grujić 1993; Fig. 8C). By further contraction, the interference pattern became suppressed and in places obliterated by dominance of SW–NE trending brachyfolds constricted within the tight imbricates of the Manín Unit.

The model depicted in Fig. 8 was developed by simple stepwise retro-deformation of the final state 8C. First the contorted lines (folded bedding traces) in the NW–SE cross-section were restored to a straight horizontal position in Fig. 8B, which gave approximately 37.5 % of horizontal shortening between steps B and C. Then shortening in the SW–NE section was restored in the same way to the initial state in Fig. 8A after 10 % of horizontal extension. In an alternative, single-phase model, the phase (B in Fig. 8) would be omitted and the block in the initial state (A) would have the same unit length of 25 km as in the final state (C).

Summing up, we infer that particularly the last two phenomena, namely the thickness variations in the competent Urgonian layer and the pre-existing, NW–SE to N–S trending macroscopic folds, played a decisive role in nucleation and then amplification of the Butkov pericline (Fig. 8). After reaching the maximum possible contraction solely by flexural-slip folding, further shortening was achieved by NW-verging reverse faulting and imbrication of the folded strata complexes of the Manín Unit. Shortening progressed under the constantly NW–SE to NNW–SSE oriented compression also during the subsequent brittle deformation stages producing systems of subvertical conjugate strike slips that truncate the whole strata successions, and smaller-scale, mostly NW-dipping backthrusts.

Timing, duration and rate of deformation

The age relationships of the structural evolution of the Manín and adjacent units can only be deduced from overprinting criteria and from the sedimentary record. As summarized by Plašienka & Soták (2015 and references therein), the nappe emplacement of the Manín Unit should have occurred at the same time as the other Fatric (Krížna) units of the CWC, presumably during the latest Turonian. Afterwards, the Manín and Klape units became constituents of the accretionary wedge at the leading edge of the CWC orogenic system, where they were subjected to alternating contraction and distension events related to the supercritical vs. subcritical taper geometry, respectively, as the wedge grew by frontal accretion of the PKB Oravic units during the Senonian, and the EWC Magura units during the Paleogene. The shortening stages are recorded by shallowing of sedimentary environments, expansion of marginal patch reefs, input of coarse clastic material into the foredeep and wedge-top basins, and uplift and erosion of intra-basinal, fold-thrust elevations. Extension and wedge collapse stages are recorded by deepening of sedimentary basins and unification of deep-water hemipelagic conditions (e.g., the Campanian couches-rouges facies). In the Manín Unit, this development is registered by the Senonian strata of the Podmanín Group (Fig. 1), filling up the Lieskov–Praznov and Hlboké synforms (Plašienka & Soták 2015). Yet the latest Cretaceous (late Campanian–Maastrichtian) deposits reflect regression, hence they can be possibly considered as the growth strata related to the along-strike contraction and the SW–NE to W–E contraction event, as well as early stages of the NW–SE oriented shortening.

As the Western Carpathian orogenic wedge progressively grew by frontal accretion of the PKB Oravic units in the latest Cretaceous and Paleocene, and then by accretion of the Magura units of the External Carpathian Flysch Belt during the Eocene and Oligocene, the Manín Unit was gradually shifted from the toe to the overthickened rear of the wedge. In this backstop position, the Manín Unit was strongly compressed and shortened horizontally with development of the conspicuous macrofold structures. During the Early Miocene, protracting contraction triggered additional tightening and restricted backthrusting and transpression between the CWC rigid buttress and the External Carpathian accretionary wedge (e.g., Plašienka & Soták 2015; Šimonová & Plašienka 2017).

Assuming this scenario, the main shortening phase with growth of the Butkov and other macrofolds in the Manín Unit likely occurred in the Paleocene times, still before the Early Eocene collapse phase and transgression of the Súľov Fm. (Soták et al. 2017). The Lower–Middle Eocene deposits of the Súľov Fm. are located in independent structures to the east of the investigated area (Fig. 1). The time interval Danian–Thanetian implies maximum 10 Ma duration for development of the Butkov and similar anticlines, which is in line with both the theoretical models and direct observations on syn-sedimentary large-scale growth structures (e.g., Suppe et al. 1992; Butler & Lickorish 1997; Vergés et al. 2002; Nemčok et al. 2005). Substantially higher fold amplification rates, of ~1 Ma duration only, and the forward slip velocity of 1 cm per year were detected by magnetostratigraphic investigations of growth strata in frontal anticlines of the Zagros Mts. (Ruh et al. 2014a). This might be explained by the very weak basal detachment made of evaporites, unconstrained foreland, and generally weak rheology of the folded succession. Nevertheless, our 10 Ma fold growth estimate is the maximum, it might have been considerably less, but available stratigraphic data do not allow a better resolution. Therefore we tentatively assume the 5–10 Ma growth period for the Butkov and other macrofolds in the Manín Unit.

For the 37.5 % modelled gross contraction of the presently 5 km wide belt of the Manín Unit in the Butkov area (Fig. 8C), the 5–10 Ma folding period would mean 0.6–0.3 mm yr^{-1} shortening velocity in average. The resulting bulk strain would be ε=0.375 (as the ratio of the original vs. present length difference and the initial length) achieved at the rate $\dot{\varepsilon} = 2.4$ to 1.2×10^{-15} s^{-1} for the 5–10 Ma time interval. More specifically, considering the restoration of the outcropped part of the Butkov anticline solely (Fig. 9), the horizontal shortening amounts to ca. 1 km and the average shortening-slip velocity would be then about 0.2–0.1 mm yr^{-1} only. The restoration results in the calculated finite strain ε=0.333 and the strain rate $\dot{\varepsilon} = 2.1–1.0 \times 10^{-15}$ s^{-1} for the 5–10 Ma time interval. Accordingly, large-scale anticlines strengthened by a thicker strong layer seem to have grown more slowly and shortened a bit less than surrounding areas.

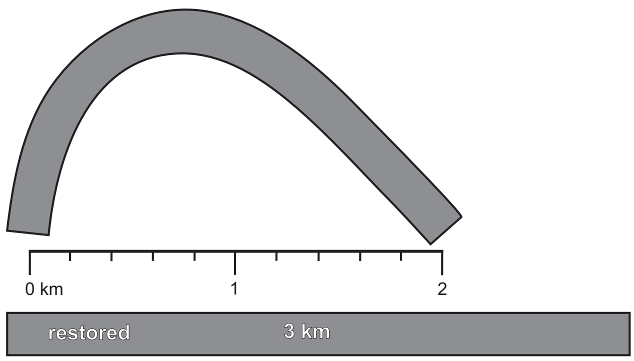

Fig. 9. Fairly simplified cross-sectional geometry of the outcropped part of the Butkov anticline represented by the buckled competent Urgonian limestone layer. The horizontal base line connects approximately the fold inflection points of the median line of the layer; thus the depicted fold width is ca. 2 km and amplitude up to 1 km. The restored competent layer would be then ~3 km wide and resultant shortening reaches 1 km corresponding to 33 %. See further details in the text.

These figures generally comply with the geologically reasonable values, although they are at the lower limit of the common estimates for both the deformation velocities and strain rates in accretionary prisms (e.g., Pfiffner & Ramsay 1982; Platt 1986; Dahlen & Suppe 1988; Mannu et al. 2016). The current shortening rates in orogenic belts range between 5 and 15 mm yr^{-1} and the plate tectonic velocities can reach as much as 50–120 mm per year, hence the bulk strain rates over orogenic belts could attain up to 10^{-12} s^{-1} (Foster & Gray 2007 and references therein). Nevertheless, much of this deformation is realized by displacements along faults and shear zones, dominantly at the sole of detached fold-thrust belts and orogenic wedges, whilst only a fraction of convergence is accomplished by internal deformation of the wedge material (Butler & Lickorish 1997).

In contrast, data obtained from kinematic or numerical modelling commonly indicate slow strain rates in the order of 10^{-15} s^{-1} or less within the low-strain domains of accretionary wedges (e.g., Plesch & Oncken 1999; Mouthereau et al. 2009; Ruh et al. 2014b). On the other hand, deformation in accretionary orogens may occur in short pulses lasting a few Ma under elevated transient strain rates reaching 10^{-14} s^{-1} or higher (Foster & Gray 2007). These variable values document dependence of mechanical behaviour of thrust wedges on a number of preconditions, such as the convergence velocity and shortening rate, strong vs. weak mechanical properties of the wedge and its sole thrust, domainal partitioning of deformation, its duration etc. In any case, our displacement and strain rate estimates for the Butkov domain and entire Manín Unit should be considered as tentative only, based on feebly constrained approximations.

Summing up, our tentative calculations imply that the Manín Unit with the Butkov and similar macrofold structures represents a low-strain and low-velocity, comparatively mechanically strong, possibly overthickened domain in the rear part of the developing accretionary wedge. Accordingly, the Manín–Butkov domain might have occupied a position of the rigid buttress that supported the supercritical wedge taper during the Paleocene, as it was inferred by Plašienka & Soták (2015).

Conclusions

The Manín Unit is a tectonic element cropping out at the boundary of the Central Western Carpathians and the Pieniny Klippen Belt in western Slovakia. Its structure is characterized by a system of non-cylindrical macrofolds, both synclinal and anticlinal, which deform the well-bedded Jurassic–Cretaceous sedimentary succession. The Butkov pericline is a prominent example of such structures. Thanks to several large quarries, its geometry is well recognized and its cross-sectional shape was depicted in numerous works. In general, the core of the Butkov pericline forms a west-east stretching elliptical dome framed by an up to 100 metres thick layer of relatively competent Urgon-type limestones (Aptian–early Albian). The anticline has a closed geometry with 60° interlimb angle and it is asymmetrical with a steeply NW dipping northern and moderately SE dipping southern limb. Internally, bedding is dipping obliquely to the general W–E trend of the Butkov anticline hinge. This discrepancy is caused by a system of NNW–SSE trending transversal tear faults, which were reactivated as eastward-stepping dextral strike-slips later, whereby individual segments of the Butkov fold were aligned in a roughly W–E direction.

Macrofolds in the Manín Unit originated by layer-parallel shortening attained by two main mechanisms — flexural slip in the well-bedded sedimentary multilayer, and buckling of a thick competent layer formed by the Urgonian limestone complex. Anticlines nucleated and then grew as domed structures from the very beginning, what is indicated by sets of superimposed, bedding-parallel slickenlines. The oldest set developed as parallel to the pericline axis at its ends, while new slickenlines are oblique as the pericline grew and the points were gradually shifted from the pericline ends to its centre. The youngest slickenlines constantly originated as perpendicular to the long pericline axis.

It is inferred that nucleation and development of brachyfolds in the Manín Unit was controlled by two main factors: (i) pre-existence of gentle macrofolds with NW–SE to N–S axial trends, which were later modified by the dominant NW–SE shortening and growth of brachyanticlines and brachysynclines as a result of interference of two perpendicular macrofold systems; (ii) lateral and longitudinal thickness variations of the Urgon limestone layer that produced buckling instabilities and initial differences in fold wavelengths leading to non-cylindricity of macrofolds amplified by protracted layer-parallel shortening and upright flexural folding. The alternative single-phase folding is considered less probable.

Acknowledgements: The paper represents a scientific output of the research projects APVV-0212-12 and APVV-16-0146. Financial support from the Slovak Research and Development Agency is gratefully acknowledged. Alex Lačný is thanked for the field assistance. Special thanks go to the reviewers Edyta Jurewicz, László Fodor and Petr Jeřábek for their constructive remarks that have substantially improved the earlier version of the manuscript.

References

Andrusov D. 1938: Étude géologique de la zone des Klippes internes des Carpathes Occidentales, III[e] partie: Tectonique. *Rozpravy Státního geologického ústavu ČSR* 9, 1–135.

Andrusov D. 1968: Grundriss der Tektonik der Nördlichen Karpaten. *Verlag der Slowakischen Akademie der Wissenschaften*, Bratislava, 1–188.

Andrusov D. 1974: The Pieniny Klippen Belt. In: Maheľ M. (Ed.): Tectonics of the Carpathian-Balkan regions. *Dionýz Štúr Geological Institute*, Bratislava, 145–158.

Beidinger A. & Decker K. 2016: Paleogene and Neogene kinematics of the Alpine–Carpathian fold-thrust belt at the Alpine–Carpathian transition. *Tectonophysics* 690, 263–287.

Beidinger A., Decker K., Zamolyi A. & Lee E.Y. 2011: Deciphering polyphase deformation in the Žilina segment of the Pieniny Klippen Belt (Steny ridge, NW Slovakia). Abstracts of the 9th CETeG meeting. *Travaux Géophysiques* 40, 5.

Birkenmajer K. 1986: Stages of structural evolution of the Pieniny Klippen Belt, Carpathians. *Studia Geologica Polonica* 88, 7–32.

Borza K., Michalík J. & Vašíček Z. 1987: Lithological, biofacial and geochemical characterization of the Lower Cretaceous pelagic carbonate sequence of Mt. Butkov (Manín Unit, Western Carpathians). *Geologický zborník — Geol. Carpath.* 38, 323–348.

Bučová J. 2013: Geological structure and structural development of the western part of the Klippen Belt. *PhD thesis, Comenius University in Bratislava*, 1–147 (in Slovak).

Butler R.W.H. & Lickorish W.H. 1997: Using high-resolution stratigraphy to date fold and thrust activity: examples from the Neogene of south-central Sicily. *J. Geol. Soc., London* 154, 633–643.

Dahlen F.A. & Suppe J. 1988: Mechanics, growth, and erosion of mountain belts. *Geol. Soc. Am. Spec. Pap.* 218, 161–178.

Dubey A.K. & Cobbold P.R. 1977: Noncylidrical flexural slip folds in nature and experiment. *Tectonophysics* 38, 223–239.

Fekete K., Soták J., Boorová D., Lintnerová O., Michalík J. & Grabowski J. 2017: An Albian demise of the carbonate platform in the Manín Unit (Western Carpathians, Slovakia). *Geol. Carpath.* 68, 5, 385–402.

Foster D.A. & Gray D.R. 2007: Strain rate in Paleozoic thrust sheets, the western Lachlan Orogen, Australia: Strain analysis and fabric geochronology. *Geol. Soc. Am. Spec. Pap.* 433, 349–368.

Grujić D. 1993: The influence of initial fold geometry on Type-1 and Type-2 interference patterns — an experimental approach. *J. Struct. Geol.* 15, 3–5, 293–307.

Jones R.R., Holdsworth R.E., Clegg Ph., McCaffrey K. & Tavarnelli E. 2004: Inclined transpression. *J. Struct. Geol.* 26, 1531–1548.

Kováč P. & Hók J. 1996: Tertiary development of the western part of Klippen Belt. *Slovak Geological Magazine* 2, 2, 136–149.

Książkiewicz M. 1977: The tectonics of the Pieniny Klippes Belt. In: Książkiewicz M., Oberc J. & Pożaryski W. (Eds): Geology of Poland, Volume 4 Tectonics. *Publ. House Wydawnictwa geologiczne*, Warsaw, 519–552.

Kysela J., Marschalko R. & Samuel O. 1982: Lithostratigraphical classification of Upper Cretaceous sediments of the Manín Unit. *Geologické práce, Správy* 78, 143–167 (in Slovak with English summary).

Liu X., Eckert A. & Connoly P. 2016: Stress evolution during 3D single-layer visco-elastic buckle folding: Implications for the initiations of fractures. *Tectonophysics* 679, 140–155.

Maheľ M. 1980: The Peri-klippen zone: nearer characterization and significance. *Mineralia Slovaca* 12, 193–207 (in Slovak with English summary).

Maheľ M. 1981: Island character of Klippen Belt; Vahicum — continuation of Southern Penninicum in West Carpathians. *Geologický zborník – Geol. Carpath.* 32, 293–305.

Maheľ M. 1983: Krížna nappe, example of polyfacial and polystructural unit. *Mineralia Slovaca* 15, 193–216 (in Slovak with English summary).

Maheľ M. 1985: Geological structure of the Strážovské vrchy Mountains. *D. Štúr Geological Institute*, Bratislava, 1–221 (in Slovak with English summary).

Maheľ M. 1986: Geological structure of the Czechoslovak Carpathians. Volume 1 — Palaeoalpine units. *Veda*, Bratislava, 1–503 (in Slovak).

Maheľ M. 1989: The Klippen Belt from the aspect of the geodynamic model. *Mineralia Slovaca* 21, 99–108 (in Slovak with English summary).

Mannu U., Ueda K., Willett S.D., Gerya T.V. & Strasser M. 2016: Impact of sedimentation on evolution of accretionary wedges: Insights from high-resolution thermomechanical modeling. *Tectonics* 35, 2828–2846.

Marko F., Vojtko R., Plašienka D., Sliva Ľ., Jablonský J., Reichwalder P. & Starek D. 2005: A contribution to the tectonics of the Periklippen zone near Zázrivá (Western Carpathians). *Slovak Geological Magazine* 11, 37–43.

Marschalko R. & Kysela J. 1980: Geology and sedimentology of the Klippen Belt and Manín Unit between Žilina and Považská Bystrica. *Západné Karpaty, séria Geológia* 6, 7–79 (in Slovak with English summary).

Márton E., Grabowski J., Plašienka D., Túnyi I., Krobicki M., Haas J. & Pethe M. 2013: New paleomagnetic results from the Upper Cretaceous red marls of the Pieniny Klippen Belt, Western Carpathians: Evidence for general CCW rotation and implications for the origin of the structural arc formation. *Tectonophysics* 592, 1–13.

Márton E., Grabowski J., Tokarski A. & Túnyi I. 2015: Palaeomagnetic results from the fold and thrust belt of the Western Carpathians: an overview. In Pueyo E.L., Cifelli F., Sussman A.J. & Oliva-Urcia B. (Eds): Palaeomagnetism in fold and thrust belts: new perspectives. *Geol. Soc. London, Spec. Publ.* 425, 7–36.

Mello J. (Ed.) 2005: Geological map of the Middle Váh River Valley 1:50,000. *Štátny geol. ústav D. Štúra*, Bratislava.

Mello J. (Ed.) 2011: Explanations to the geological map of the Middle Váh Valley 1:50,000. *Štátny geol. ústav D. Štúra*, Bratislava, 1–378 (in Slovak with English summary).

Michalík J. 1994: Lower Cretaceous carbonate platform facies, Western Carpathians. *Palaeogeogr. Palaeoclimatol. Palaeoecol.* 111, 263–277.

Michalík J. 2007: Sedimentary rock record and microfacies indicators of the latest Triassic to mid-Cretaceous tensional development of the Zliechov Basin (Central Western Carpathians). *Geol. Carpath.* 58, 5, 443–453.

Michalík J. & Vašíček Z. 1987: Geology and stratigraphy of the Butkov Lower Cretaceous limestone deposits, Manín Unit, Middle Váh Valley (Western Slovakia). *Mineralia Slovaca* 19, 115–134 (in Slovak with English summary).

Michalík J., Lintnerová O., Reháková D., Boorová D. & Šimo V. 2012: Early Cretaceous sedimentary evolution of a pelagic basin margin (the Manín Unit, central Western Carpathians, Slovakia). *Cretaceous Res.* 38, 68–79.

Michalík J., Vašíček Z., Boorová D., Golej M., Halásová E., Hort P., Ledvák P., Lintnerová O., Měchová L., Šimo V., Šimonová V., Reháková D., Schlögl J., Skupien P., Smrečková M., Soták J. & Zahradníková B. 2013: The Butkov Hill — a stone archive of Slovakian mountains and the Mesozoic sea life history. *Veda*, Bratislava, 1–164.

Mišík M. 1966: Tentative microscopical classification of veinlets in limestones (based on the Tithonian and Neocomian limestones of the Manín group of the West Carpathians). *Geologický sborník* 17, 337–344.

Mouthereau F., Fillon C. & Ma K.-F. 2009: Distribution of strain rates in the Taiwan orogenic wedge. *Earth Planet. Sci. Lett.* 284, 361–385.

Nemčok M., Schamel S. & Gayer R. 2005: Thrustbelts. Structural architecture, thermal regimes, and petroleum systems. *Cambridge University Press*, Cambridge etc., 1–541.

Neumayr M. 1871: Jurastudien. 5. Das Pieninische Klippenzug. *Jahrbuch der kaiserlich-königlichen geologischen Reichsanstalt* 21, 4, 451–536.

Odonne F. & Vialon P. 1987: Hinge migration as a mechanism of superimposed folding. *J. Struct. Geol.* 9, 7, 835–844.

Pešková I., Hók J., Potfaj M. & Vojtko R. 2012: Structural interpretation of the Varín and Orava segment of the Klippen Belt. *Geologické práce, Správy* 120, 51–64 (in Slovak with English abstract).

Pfiffner O.A. & Ramsay J.G. 1982: Constraints on geological strain rates: Arguments from finite strain states of naturally deformed rocks. *J. Geophys. Res., Solid Earth* 87, 311–321.
Plašienka D. 1983: Geological structure of the Tuhár Mesozoic (Central Slovakia). *Mineralia Slovaca* 15, 49–58 (in Slovak with English summary).
Plašienka D. 1993: Structural pattern and partitioning of deformation in the Veporic Foederata cover unit (Central Western Carpathians). In: Rakús M. & Vozár J. (Eds): Geodynamic model and deep structure of the Western Carpathians. *D. Štúr Institute of Geology*, Bratislava, 269–277.
Plašienka D. 1995a: Cleavages and folds in changing tectonic regimes: the Veľký Bok Mesozoic cover unit of the Veporicum (Nízke Tatry Mts., Central Western Carpathians). *Slovak Geological Magazine* 1, 2, 97–113.
Plašienka D. 1995b: Origin and structural position of the Upper Cretaceous sediments in the northern part of the Považský Inovec Mts. Part 2: Structural geology and paleotectonic reconstruction). *Mineralia Slovaca* 27, 179–192 (in Slovak with English summary).
Plašienka D. 1999: Tectonochronology and paleotectonic evolution of the Central Western Carpathians during the Jurassic and Cretaceous. *Veda*, Bratislava, 1–127 (in Slovak with English summary).
Plašienka D. 2012a: Jurassic syn-rift and Cretaceous syn-orogenic, coarse-grained deposits related to opening and closure of the Vahic (South Penninic) Ocean in the Western Carpathians — an overview. *Geol. Quarterly* 56, 601–628.
Plašienka D. 2012b: Early stages of structural evolution of the Carpathian Klippen Belt (Slovakian Pieniny sector). *Mineralia Slovaca* 44, 1–16.
Plašienka D. & Marko F. 1993: Geological structure of the middle part of the Považský Inovec Mts. (Western Carpathians). *Mineralia Slovaca* 25, 11–22 (in Slovak with English summary).
Plašienka D. & Soták J. 2001: Stratigraphic and tectonic position of Carboniferous sediments in the Furmanec Valley (Muráň Plateau, Central Western Carpathians). *Mineralia Slovaca* 33, 29–44.
Plašienka D. & Soták J. 2015: Evolution of Upper Cretaceous–Paleogene synorogenic basins in the Pieniny Klippen Belt and adjacent zones (Western Carpathians, Slovakia): tectonic controls over a growing orogenic wedge. *Annales Societatis Geologorum Poloniae* 85, 43–76.
Platt J.P. 1986: Dynamics of orogenic wedges and the uplift of high-pressure metamorphic rocks. *Geol. Soc. Am. Bull.* 97, 1037–1053.
Plesch A. & Oncken O. 1999: Orogenic wedge growth during collision — constraints on mechanics of a fossil wedge from its kinematic record (Rhenohercynian FTB, Central Europe). *Tectonophysics* 309, 117–139.
Price N.J. & Cosgrove J.W. 1990: Analysis of geological structures. *Cambridge University Press*, 1–520.
Prokešová R., Plašienka D. & Milovský R. 2012: Structural pattern and emplacement mechanisms of the Krížna cover nappe (Western Carpathians, Slovakia). *Geol. Carpath.* 63, 13–32.
Rakús M. 1997: Manín gorge. *Excursion Guide, Internat. Conference Alpine evolution of the Western Carpathians and related areas*, Bratislava, Sept. 11–14, 1997, 6–11.
Rakús M. & Hók J. 2005: The Manín and Klape units: Lithostratigraphy, tectonic classification, paleogeographic position and relationship to Váhicum. *Mineralia Slovaca* 37, 9–26 (in Slovak with English summary).
Ramsay J.G. 1967: Folding and fracturing of rocks. *McGraw-Hill*, New York, 1–568.
Ramsay J.G. & Huber M.I. 1983: The techniques of modern structural geology. Vol. 1: Strain analysis. *Academic Press*, London etc, 1–307.
Ramsay J.G. & Huber M.I. 1987: The techniques of modern structural geology. Vol. 2: Folds and fractures. *Academic Press*, London etc, 1–700.
Ratschbacher L., Frisch W., Linzer H.-G., Sperner B., Meschede M., Decker K., Nemčok M., Nemčok J. & Grygar R. 1993: The Pieniny Klippen Belt in the Western Carpathians of northeastern Slovakia: structural evidence for transpression. *Tectonophysics* 226, 471–483.
Ruh J.B., Hirt A.M., Burg J.-P. & Mohammadi A. 2014a: Forward propagation of the Zagros Simply Folded Belt constrained from magnetostratigraphy of growth strata. *Tectonics* 33, doi:10.1002/2013TC003465.
Ruh J.B., Gerya T. & Burg J.-P. 2014b: 3D effects of strain vs. velocity weakening on deformation patterns in accretionary wedges. *Tectonophysics* 615–616, 122–141.
Ruh J.B., Gerya T. & Burg J.-P. 2017: Toward 4D modeling of orogenic belts: Example from the transpressive Zagros Fold Belt. *Tectonophysics* 702, 82–89.
Salaj J. 2006: Microbiostratigraphy of the Gosau development in the Klape Unit, Western Carpathian Paleoalpine accretionary belt. *Mineralia Slovaca* 38, 1–6.
Sanderson D.J. & Marchini W.R.D. 1984: Transpression. *J. Struct. Geol.* 6, 449–458.
Scheibner E. 1961: The tectonic style of the Klippen Belt and the idea about its origin. *Geologický sborník* 12, 2, 153–158.
Schmalholz S.M. 2008: 3D numerical modeling of forward folding and reverse unfolding of a viscous single-layer: Implications for the formation of folds and fold patterns. *Tectonophysics* 446, 31–41.
Soták J., Pulišová Z., Plašienka D. & Šimonová V. 2017: Stratigraphic and tectonic control of deep-water scarp accumulation in Paleogene synorogenic basins: a case study of the Súľov Conglomerates (middle Váh Valley, Western Carpathians). *Geol. Carpath.* 68, 5, 403–418.
Storti F., Soto Marín R., Rossetti F. & Casas Sainz A.M. 2007: Evolution of experimental thrust wedges accreted from along-strike tapered, silicone-floored multilayers. *J. Geol. Soc., London* 164, 73–85.
Stur D. 1860: Bericht über die geologische Uebersichts-Aufnahme des Wassergebietes der Waag und Neutra. *Jahrbuch der k.k. geologischen Reichsanstalt* 11, 17–151.
Suppe J., Chou G.T. & Hook S.C. 1992: Rates of folding and faulting determined from growth strata. In: McClay K.R. (Ed.): Thrust tectonics. *Chapman & Hall*, Suffolk, 105–121.
Šimonová V. & Plašienka D. 2011: Fault kinematics and palaeostress analysis in the Butkov quarry (Manín Unit, Western Carpathians). *Acta Geologica Slovaca* 3, 21–31 (in Slovak with English summary).
Šimonová V. & Plašienka D. 2017: Stepwise clockwise rotation of the Cenozoic stress field in the Western Carpathians as revealed by kinematic analysis of minor faults in the Manín Unit (western Slovakia). *Geol. Quarterly* 61, 1, 252–265.
Uhlig V. 1903. Bau und Bild der Karpathen. In Diener C., Hoernes R., Suess F.E. & Uhlig V. (Eds): Bau und Bild Österreichs. *F. Tempsky*, Wien und *G. Freytag*, Leipzig, 649–911.
Uhlig V. 1904: Über die Klippen der Karpathen. *Congrès Géologique International Compte Rendu de la IX. Session, Vienne 1903*, Premier Fascicule, Imprimerie Hollinek Fréres, Vienne, 427–453.
Vergés J., Marzo M. & Muñoz J.A. 2002: Growth strata in foreland settings. *Sediment. Geol.* 146, 1–9.
Žítt J. & Michalík J. 1988: Early Cretaceous phyllocrinids (Crinoidea, Cyrtocrinida) in the Manín Unit (Mt. Butkov, Middle Váh Valley, Central West Carpathians). *Geologický zborník — Geol. Carpath.* 39, 3, 353–368.